Journal of Materials and Electronic Devices 4 (2024) 24-29

Photonic behavior of ZnO nanoparticle doped MXene nanocomposite produced by hydrothermal method

Kadir DEMİRELLİ[1*], Cemile ERCAN[2], Gamze BARIM[3]

[1]Faculty of Science, Department of Chemistry, University of Firat, 23169 Elazig, Turkey
[2]Faculty of Science, Department of Chemistry, University of Firat, 23169 Elazig, Turkey
[3]Adiyaman University, Faculty of Sciences and Arts, Department of Chemistry, 02040, Adiyaman, Turkey

MXene/ZnO nanocomposite and ZnO nanoparticles were produced by hydrothermal treatment in aqueous medium at 180 ºC for 24 h. The MXene0.30/ZnO nanocomposite was prepared in ZnO matrix. The SEM-EDX analysis showed that the ZnO nanoparticles has an hexagonal wurtzite structure. MXene0.30/ZnO nanocomposite was characterized by FT-IR and SEM techniques. The photonic behavior of the MXene0.30/ZnO nanocomposite were investigated under various illuminations such as 20, 40, 60, 80 and 100 mW/cm^2. The photocurrent of the device were measured under various voltages and it was observed that the photocurrent increased with increasing voltage. Furthermore, the devices show excellent optoelectronic characteristics in the photoconductive and photovoltaic modes.

Keywords: *MXene, zinc oxide, nanocomposite, photovoltaic, hydrothermal method, interdigital electrods.*

Submission Date: 22 August 2024
Acceptance Date: 7 October2024

**Corresponding author: kdemirelli@firat.edu.tr*

1. Introduction

$Ti_3C_2T_x$ MXene, which is a new transition metal carbide material with two-dimensional layered structure and one of the MXene chemistries, is characterised by its low density, high metallic electrical conductivity, high specific surface area and tunable terminal groups, among others. The dense polar groups (-O-, -OH, -F, etc.) on the surface of $Ti_3C_2T_x$ MXene, which is a metamaterial, exhibit the task of use as active sites for other phases (metal oxides, magnetic units, polymers, etc.) to improve their polarisation behaviour [1]. Therefore, MXene is one of the interesting chemistries that have recently found their place in the field of electromagnetic wave absorption and photonic applications [2-5]. Recently, many attractive properties of MXenes, such as plasmonic behaviour and optical nonlinearity, have been demonstrated and successfully applied in various optical and optoelectronic devices. In order to realise the full potential of MXenes for photonic applications, a new group of researchers has begun to emerge who are

investigating its undiscovered properties. With the versatility of the available compositions and their outstanding optical properties, MXenes are known to have the potential to facilitate the development of many new tunable nanophotonic devices [6].

Recently, many attractive properties of MXenes, including plasmonic behaviour, optical nonlinearity and highly efficient photothermal conversion, have been demonstrated, enabling their successful use in various optical and optoelectronic devices. With MXene and some of its composites having versatile and superior optical properties, MXenes have been suggested to have the potential to

facilitate the development of many new tunable photonic or nanophotonic devices [7]. MXene's polar functional groups such as oxygen, fluorine, hydroxyl as terminal groups not only determine its hydrophilic properties, but also affect its electrochemical properties such as being negatively charged, ion adsorption and diffusion, as well as its electronic properties [8]. MXenes have excellent light absorption capacity across the entire solar spectrum [9]. The light-to-heat conversion performance of Ti_3C_2Tx MXene upon exposure to light indicates the potential of MXene to generate heat by itself. This behavior can be attributed to the electronic transitions of free electrons on the MXene surface. In this context, the surface temperature of the skin coated with Ti_3C_2Tx/polyacrylate composite was at least 5 °C higher than that of the skin coated with Ti_3C_2Tx/polyacrylate composite compared to the exposure of only polyacrylate-coated skin to sunlight [10].

This study reveals the response of the prepared MXene Ti3C2Tx nanocomposite to different illumination intensities. For this purpose, the study focuses on the photonic behaviour of nanocomposites prepared with ZnO nanoparticle doped MXene, which has not been encountered in the literature before.

2. Experimental

2.1. Materials and analytical techniques

Sodium hydroxide (NaOH) and zinc acetate [$Zn(CH_3COO)_2.2H_2O$] purchased from Across were used in the synthesis of ZnO nanoparticles. Ti_3AlC_2 MAX was used as a precursor for the preparation of Ti_3C_2Tx MXene nanoflakes. Ti_3AlC_2 (MAX phases, ≤ 100 nm), hydrofluoric acid (HF for 48% soln, d=1.15 g/mL, Merck) were used as received.

The characterization of MXene0.30/ZnO nanocomposite was confirmed by FT-IR ATR spectroscopy using (Thermo Scientific Nicolet IS5) at range of 4000–400 cm^{-1}. SEM and EDX measurements were performed with BAUM ZEISS Sigma 300 FESEM (Field Emission Scanning Electron Microscope). The interdigital contact has the interdigital channels that contains two different metal electrodes. The electrode used in this work contains 57 interdigitals and have 75 μm between contacts and 35 μm contact thickness. The electrical characterization of the MXene0.30/ZnO nanocomposite was performed using a Fytronix electronic device characterisation system including AAA Class Solar Simulator and FY-9000 Sourcemeter.

2.2. Synthesis of ZnO nanoparticles

To synthesis ZnO nanoparticles, aqueous solution of $Zn(CH_3COO)_2.2H_2O$ (0.6 M) was prepared by stirring in 15 ml of deionised water. In another beaker, the solution of 10 ml of NaOH (1.2 M) solution was prepared within deionised. Both of solutions were transferred to teflon coated sealed stainless steel autoclave and kept at 180 °C for 24 hours under around 10 atm pressure. It was then allowed to cool naturally to room temperature. After the reaction was complete, the resulting white solid products were washed with methanol, filtered, and then dried in air in a laboratory oven at 60 °C.

2.3. Preparation of $Ti_3C_2T_x$ (MXene)

According to the procedure described in the literature [11], HF(aq) used as an etch was diluted from 40% HF (Merck) solution to the desired concentration of 18% (v/v). From the diluted 18% (v/v) HF solution, 28 ml of HF(aq) was placed in a plastic container where the reaction would take place. Then, 1 g of Ti_3AlC_2 MAX phase was added stepwise to the reaction vessel. The reaction was then carried out at 50 °C for 24 h with magnetic stirring. The resulting solution was washed with water and alcohol until neutralised. The mixture was then sonicated under nitrogen gas for about 30 min. After this process, the suspension solution was filtered by vacuum filtration. Upon completion of filtration, black coloured MXene was dried under vacuum at 65 oC for one day under vacuum. MXene was then stored in the dark.

2.4. Synthesis of MXene $Ti_3C_2T_x$/ZnO nanocomposite

MXene/ZnO nanocomposites were prepared by producing ZnO nanoparticles in presence of MXene by hydrothermal method. For this purpose, 80 Mg of MXene was placed in 15 mL deionised water in a clean container and sonicated for 2 hours. At the same time, to produce ZnO nanoparticles in MXene medium, $Zn(CH_3COO)_2.2H_2O$ (0.6 M) aqueous solution was prepared in 15 mL deionised water in a second beaker and NaOH (1.2 M) solution was prepared in 10 mL water in a third beaker. The three solutions were transferred to teflon coated sealed stainless steel autoclaves and kept at 180 °C for 12 hours under about 10 atm pressure. They were then allowed to cool naturally to room temperature. The resulting black solid products were washed with deionised water and precipitated by centrifugation. The precipitated product was washed again with deionised water and precipitated by centrifugation. This process was repeated until pH = 7. Then, it was left to dry in a vacuum oven 24 set at 60 °C.

3. Results and Discussion

Fig. 1 indicates FT-IR spectrum of MXene0.30/ZnO nanocomposite in the 4000– 400 cm^{-1} range. The formation of ZnO nanoparticles was evident from the

appearance of peaks at 689 - 991 cm^{-1} region [12]. One of the most prominent bands of MXene's surface functional groups was observed at 3453 cm^{-1} due to hydrogene-bonding to hydroxyl group or water molecule. The sharp band at 3620 cm^{-1} has been attributed to free oxygen–hydrogen stretching in the water molecules [13]. As indicated in Fig. 1. One of the striking places in the spectrum is the change in the 1900-2310 cm^{-1} region. The terminations on the surface of the MXene have strong physical interactions due to containing functional groups such as -OH, –F and -O-. So, the band seen between 1900 and 2310 cm^{-1} region were evidence of the presence of polar OH groups as one of terminal groups on the surface of MXene. Especially, the important band at 2222 cm^{-1} was estimated to be due to a combination of hydronium (H_3O^+) bending and rotation [14]. In this regards, FT-IR analyses indicated that he presence of medium intensity bands of the water cluster proton (hydronium) in the region 1800-2400 cm^{-1} was due to the confinement of protons in MXene interlayers [15].

Typical SEM images signifies the pure ZnO and MXene0.30/ZnO nanoparticles composite are shown in Fig. 2(a-c). The micro structure formed exhibited uniform and compact structure, interconnected by grains. When the SEM image of the pure ZnO as seen in Fig. 2a was examined, it is seen that the ZnO nanoparticles produced generally have a hexagonal morphological structure. Fig. 2b shows the qualitative elemental analysis results performed using energy dispersive X-ray (EDX) analysis for ZnO nanoparticles. Clear peaks were shown by the EDX spectrum corresponding to Zn and O elements. The image of SEM in the Fig. 2c shows that ZnO nanoparticles are present in MXene nanosheets and have a rough surface, while it also reveals the presence of ZnO NPs with hexagonal morphology interspersed on MXene nanosheets. It forms a heterogeneous but potentially well-dispersed structure as shown in Fig. 2c.

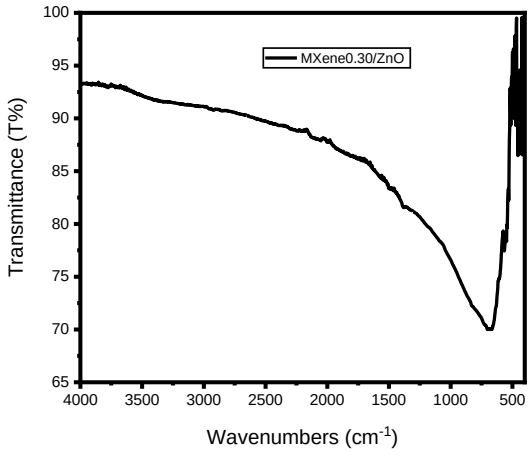

Fig.1. FT-IR spectrum of MXene0.30/ZnO nanocomposite

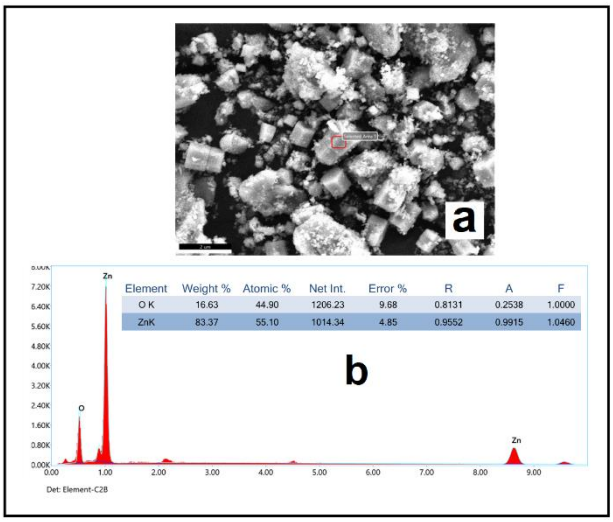

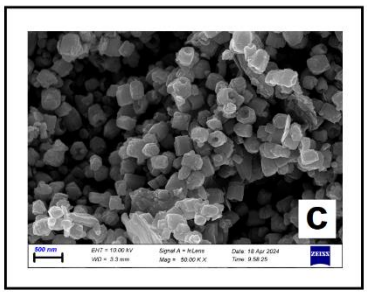

Fig. 2. SEM image a) ZnO b) EDX of ZnO and c) SEM image of MXene0.30/ZnO nanocomposite

3.2. Photonic behaviors of MXene/ZnO nanocomposites

Functional groups on the MXene surface show a significant effect on the stability, electrical behavior, electronic structure and other physical and chemical properties of MXene [16]. Therefore, the controllable arrangement of MXene surface functional groups can be considered as an important requirement for obtaining MXene materials with different properties.

The photocurent-voltage curves under 20, 40, 60, 80 and 100 mW/cm^2 illumination conditions of MXene0.30/ZnO nanocomposite prepared on the interdigital electrods with electrode spacing of 5 μm were plotted as in Fig. 3(a). Under illumination, the forward current of MXene0.30/ZnO nanocomposite increased in a nanolinear behavior as the illumination intensity increased. If the frequency of the light is greater than the threshold value the photocurrent increases and it depends on the intensity of the light. In this regards, as the intensity of the light falling on the nanocomposite increases, the current has increased. So, it is suggested that the effect of MXene is great in the increase of forward current with increasing voltage in MXene0.30/ZnO nanocomposite. Also, because the excitation binding energy of MXene is large, dissociation

occurs with increasing voltage and this behavior is a reason for the increase in forward photocurrent. Fig. 3(b) shows the photocurent-voltage plot of pure MXene. When the photocurent-voltage measurements of pure MXene and MXene0.30/ZnO nanocomposite were compared with those of pure MXene, it was observed that the nanocomposite was more sensitive to light and the photocurrent increased with increasing voltage. While the current value of MXene at 1.0 V changes from 21 nA to 82 nA, it changes from 3.18 mA to 6.06 mA in MXene0.30/ZnO nanocomposite.

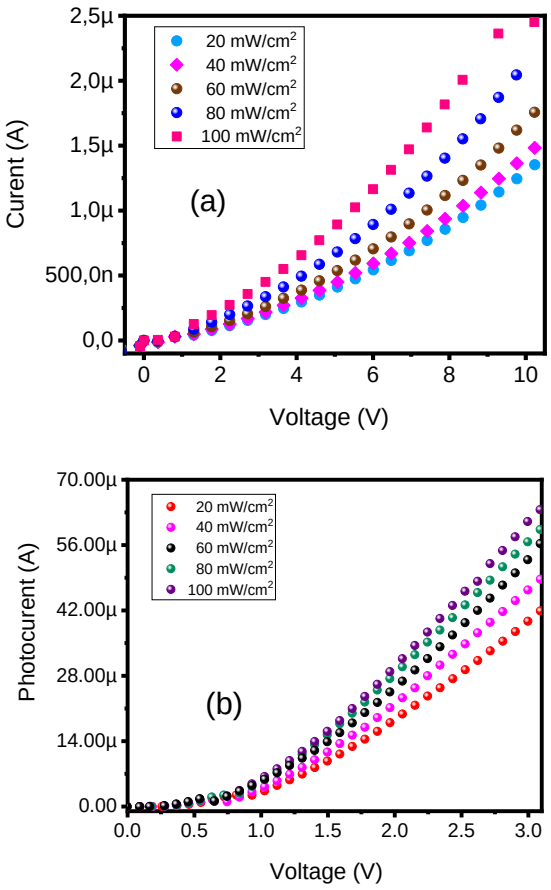

Fig. 3. (a) photocurent-voltage characteristics of device with 5 µm electrode spacing under various illumination conditions of MXene0.30/ZnO nanocomposite b) photocurent-voltage characteristics of neat MXene $Ti_3C_2T_x$

The photocurent-voltage graph at the illumination intensities is shown Fig. 4(a) with logI-logV representation. The increase in applied voltage at various light intensities for the current-voltage graph can be attributed to the increasing effect of diffusion current. It can also be attributed to the recombination of electrons and holes in the depletion region of junctions in this voltage range. It also shows the increase in the number of electrons excited by exposure of the nanocomposite to light intensities of between 20 and 100 mW/cm^2. When the frequency of the incident light matches the resonant frequency of MXenes' surface electrons, the electric field of the incident light can resonate with MXenes' surface electrons and excite the resonant vibration mode of the surface. The electrical field generated by this resonant vibrational mode then interacts with the incident light to create a localized region of electromagnetic field enhancement called the plasmon resonance region electrons [17, 18]. For light intensities from 20 mW/cm^2 to 100 mW/cm^2, the slopes were determined by the linear change observed from the as given in Fig. 4(a) plot of logI vs. logV. The slope values were found to vary from 1.51 to 1.96. Slope values greater than one indicate a continuous or nearly continuous distribution of impurity states localised in the forbidden energy range. These values confirm that the nanocomposite has a photoconductive mechanism. When the line slopes recorded for region I of Fig. 4(a) are plotted against the light intensity, the slope values exhibit a nonlinear behaviour as seen in Fig. 4(b).

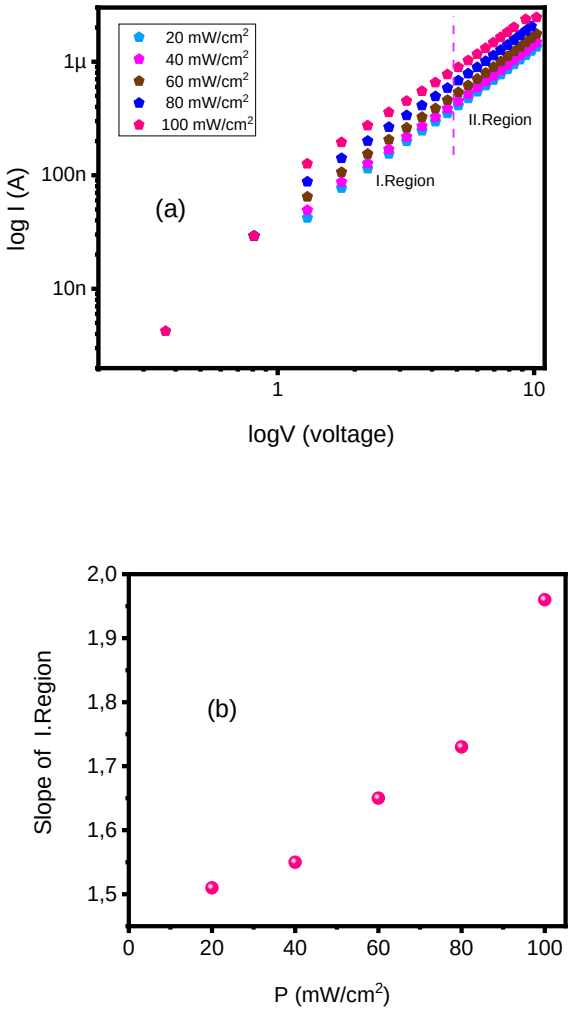

Fig. 4. Graphs of a) logI versus logV b) slope of I. region versus P for MXene0.30/ZnO nanocomposite

Table 1. Slopes of I. and II. Regions from graph of logI vs. logV for MXene0.30/ZnO nanocomposite

Regions	20 mW/cm²	40 mW/cm²	60 mW/cm²	80 mW/cm²	100 mW/cm²
I. Region	1.51	1.55	1.65	1.73	1.96
II. Region	1.69	1.61	1.69	1.67	1.61

The I_{ph} and P_{ph} graphs of the nanocomposite are shown in Fig. 3. The photocurrent as a function of the illumination power density is shown and corresponds to four states of the device at four different voltages. Iph versus Pph measurements of the nanocomposite at different voltages were performed. The photocurrent mechanism of the MXene0.30/ZnO nanocomposite was analysed by equation 1 (Eq. 1),

$$I_{ph}=BP^{m} \quad (1)$$

here I_{ph} is the photocurrent, P_{ph} is the light intensity and B is a constant. From Fig. 5, it can be seen that each of the three data sets follows an approximately straight line, indicating that the luminous intensity and illumination power are linked by a power law. The photocurrent of nanocomposite mechanism clearly shows a nonlinear behaviour as seen in Fig. 5. The nanocomposite material prepared on the interdigital contact exhibits a photosensitive behaviour. As can be seen from the I_{ph}-P_{ph} graphs plotted at various voltages, the photocurrent values increased with increasing voltage. For 100 mW/cm^2 light intensity, the photocurrent values at 2V, 4V, 6V and 10V voltages were 610 nA, 1.16 µA, 1.83 µA and 2.11 µA, respectively. When Ti_3C_2Tx MXene0.30/ZnO nanocomposite is exposed to both light intensity and voltage, the amount of charge carriers generated increases and then current is generated due to the presence of free electrons. With the decrease in the amount of electrons, the photocurrent decreases.

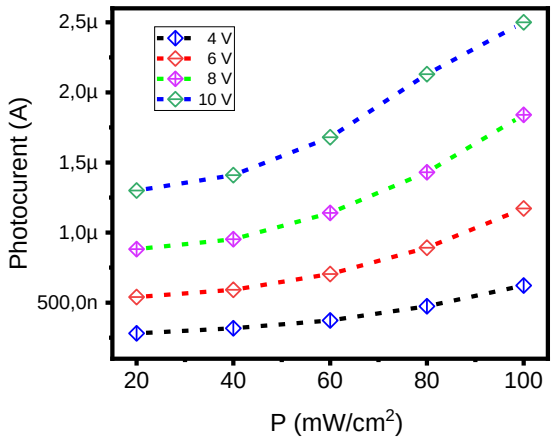

Fig. 5. I_{ph} versus P_{ph} plot of MXene0.30/ZnO nanocomposite at various voltages

4. Conclusion

MXene0.30/ZnO nanocomposite was characterised using FT-IR and SEM-EDX techniques. The hexagonal geometry of the hydrothermally produced ZnO was confirmed by SEM. Current-voltage measurements of the nanocomposite were performed. Photocurrent-voltage measurements were performed at different light intensities by forming a film on a nanocomposite interdigital contact and the photocurrent showed a clearly nonlinear behaviour. In this context, the nanocomposite material prepared on the interdigital contact exhibited a photosensitive behaviour. Photocurrents were measured against P at different voltages. For 100 mW/cm^2 light intensity, the photocurrents at 2V, 4V, 6V and 10V voltages were 610 nA, 1.16 µA, 1.83 µA and 2.11 µA, respectively.

Acknowledgements

The authors thank TÜBİTAK for financial support from the TÜBİTAK-2209-A (Project No: 1919B012327218) and FUBAP.23.28

References

[1] Z. Guo, P. Ren, Z. Lu, K. Hui, J. Yang, Z. Zhang, Z. Chen, Y. Jin, F. Ren, ACS Appl. Mater. Interfaces 14 (36) (2022) 41468–41480.
[2] Y. Lu, S. Zhang, M. He, L. Wei, Y. Chen, R. Liu, Carbon 178 (2021) 413–435.
[3] Z. Guo, P. Ren, J. Wang, X. Hou, J. Tang, Z. Liu, Z. Chen, Y. Jin, F. Ren, Chem. Eng. J. 451 (2023) 138667.
[4] K. Demirelli, A Çelik, Y Aksoy, M Yegin, E Barım, Ö Hanay, H Hasar, Materialwiss Werkst. 55 (2024) 1213–1226.
[5] X. Tang, M. Zhou, Journal of Physics: Energy, *3*(4) (2021) 042001.

[6] Y. I. Jhon, J. Lee, Y. M. Jhon, J. H. Lee, Nanophotonics, *10*(6) (2021) 1741–1751.

[7] D. Zhang, D. Shah, A. Boltasseva, Y. Gogotsi, ACS Photonics 9(4) (2022) 1108–1116.

[8] H. Kim, Z. Wang, H. N. Alshareef, Nano Energy 60 (2019) 179–197.

[9] Z. Li, H. Zhang, J. Han, Y. Chen, H. Lin, T. Yang, Adv. Mater. 30 (2018) 1706981.

[10] Y. Zhang, K. Ruan, Y. Guo, J. Gu, Adv. Photonics Res. 4 (2023) 2300224.

[11] M. Naguib, M. Kurtoglu, V. Presser, J. Lu, J. Niu, M. Heon, L. Hultman, Y. Gogotsi, M. W. Barsoum, Adv. Mater. 23 (2011) 4248–4253.

[12] Z. Y. Zhao, M. H. Wang, H. P. Zhang, J. Mater. Sci: Mater. Electron. 27 (2016) 1777–1782.

[13] M. Lounasvuori, Y. Sun, T. S. Mathis, L. Puskar, U. Schade, D. E. Jiang, Y. Gogotsi, T. Petit, Nat. Commun, 14 (2023) 1322.

[14] K. Demirelli, A. Dere, E. Barım, H. Tuncer, F. Yakuphanoglu, Synth. Met. 309 (2024) 117770.

[15] J. A. Fournier, C. J. Johnson, C. T. Wolke, G. H. Weddle, A. B. Wolk, M. A. Johnson, Science, 344 (6187) (2014) 1009–1012.

[16] X. Zhang, R. Lv, A. Wang, W. Guo, X. Liu, J. Luo, Angew. Chem. Int. Ed. 57 (2018)15028–15033.

[17] X. Liu, Y. Li, X. Sun, W. Tang, G. Deng, Y. Liu, Z. Song, Y. Yu, R. Yu, L. Dai, J. Shui, Matter 4 (2021) 1735.

[18] Y. Zhang, K. Ruan, Y. Guo, and J. Gu, Adv. Photonics Res. 4 (2023) 2300224.